Journal of the Serbian Chemical Society
JSCS@tmf.bg.ac.rs • www.shd.org.rs/JSCS
J. Serb. Chem. Soc. *88* (9) 889–904 (2023)
JSCS–5669
Original scientific paper
Published 9 September 2023

Bactericidal effects of copper–polypyrrole composites modified with silver nanoparticles against Gram-positive and Gram-negative bacteria

PATRICIA L. MARUCCI[1], MARIA G. SICA[1,2], LORENA I. BRUGNONI[1,3] and MARÍA B. GONZÁLEZ[4]*

[1]*Department of Biology, Biochemistry and Pharmacy, National University of the South, Bahía Blanca, Argentina,* [2]*Department of Health Sciences, National University of the South, Bahía Blanca, Argentina,* [3]*Institute of Biological and Biomedical Sciences, National University of the South, CONICET, Bahía Blanca, Argentina and* [4]*Chemical Engineering Department, Institute of Electrochemistry and Corrosion Engineering, National University of the South, CONICET, Bahía Blanca, Argentina*

(Received 13 February, revised 26 March, accepted 2 August 2023)

Abstract: The aim of this research is to study the bactericidal effects of copper––polypyrrole (PPy) composites deposited onto 316L stainless steel (SS) modified with silver nanoparticles (Np). The antimicrobial properties were evaluated against twenty-four strains of Gram-positive and Gram-negative bacteria. Among the twenty-four strains studied, isolates included reference strains (*Escherichia coli* ATCC 25922, *Escherichia coli* 0157:H7 EDL 933, *Staphylococcus aureus* ATCC 25923 and *Listeria monocytogenes* ATCC 7644), as well as strains isolated from food and clinical samples. The antimicrobial activity of the composites demonstrated that all PPy-modified films had antibacterial properties. Notably, Cu-PPyAgNp$_{500}$ exhibited the strongest inhibitory activity against both Gram-negative and Gram-positive bacteria. Surface modification of 316L SS with these films is a promising and viable alternative for the development of novel antibacterial composites that can inhibit the growth of a significant number of bacteria.

Keywords: conducting polymer; antibacterial applications; metallic nanoparticles; stainless steel.

INTRODUCTION

Antibiotic resistance is considered by the World Health Organization as a critical problem of global concern, which causes higher medical costs, prolonged hospital stays, and increased mortality.[1] This threat is caused by the overuse and abuse of antibiotics, coupled with the natural evolutionary processes of bacteria.

* Corresponding author. E-mail: belen.gonzalez@uns.edu.ar
https://doi.org/10.2298/JSC230213047M

There is a significant interest from all nations in developing a global action plan to prevent and control the growth of antibiotic resistance.[2] In the biomedical field, bacterial infections at the site of implanted medical devices such as catheters and artificial prostheses are a serious and persistent problem. Although medical implants greatly improve the patients' quality of life, implant-related infections are recognized as a tragic problem, often requiring revision surgery for individuals with severe infections.[3] To overcome this problem, surface modifications are used to improve the antibacterial properties of materials.[4,5] Some antibacterial strategies for metal implants may include inhibiting the adhesion, the colonization, the biofilm formation and the proliferation of bacteria.[6,7] Recently, many organic compounds, including conducting polymers or biopolymers, have demonstrated their potential as antibacterial and antiviral agents to combat infections caused by harmful bacteria and viruses.[8,9]

In recent years, the research on conducting polymers and their composites as antibacterial agents has gained momentum.[8,10] In particular, polypyrrole (PPy) has been successfully explored for new antibacterial systems due to its easy preparation, low cost, low toxicity and biocompatibility.[11] In a recent study, the antibacterial properties and the synergistic behavior of a composite consisting of silver nanoparticles, single-walled carbon nanotubes and PPy were reported. The prepared ternary composite exhibits the following order of performance within 24 h at a concentration of 0.048 mg/mL: *Bacillus cereus* > *Escherichia coli* > *Pseudomonas aeruginosa* > methicillin-resistant *Staphylococcus aureus*.[12] Another noteworthy composite consisting of PPy and zinc-doped copper oxide microparticles showed remarkable antimicrobial effects against *E. coli* and *S. aureus*. The authors postulated that the mechanism of cell death was mainly induced by the release of reactive oxygen species (ROS), which damage bacterial membranes, DNA and proteins.[13] Recent studies conducted in our laboratory have demonstrated that hybrid antimicrobial coating materials containing PPy combined with copper,[14,15] silver[16] or zinc[17] species have also shown great bactericidal effects.

Silver has a long history of use in pharmacology and medicine as an antibacterial agent. In the field of orthopedics, silver nanoparticles (AgNps) have yielded excellent results in modifying implant surfaces to prevent implant-related infections.[18] Furthermore, the antibiotic activity of AgNps has been studied in various bacteria, yielding positive results.[19] However, the exact mechanisms by which Ag acts as antimicrobial agent have not been fully clarified. Three hypotheses have been proposed: 1) Ag^+ are taken up by bacteria, triggering a cascade of intracellular reactions that disrupt ATP production and DNA replication; 2) silver ions promote the generation of reactive oxygen species (ROS) both inside and outside bacterial cells, causing oxidative stress and subsequent damage to bacterial membrane lipids and DNA; 3) in the case of AgNps, it is believed that

these particles can penetrate cell membranes and activate one or all of the aforementioned mechanisms.[20]

The incorporation of copper as antibacterial agent in metallic implants has also been considered.[21] The interaction between copper and bacteria cells involves several important events that can be listed as follows: The first event (A) is the accumulation of Cu ions on the bacteria membrane or within the cell. This accumulation not only causes membrane damage through depolarization, but also leads to the leakage of intracellular components; B) the generation of ROS by copper ions may lead to further cell damage; C) Cu ions inside bacterial cells may bind with DNA molecules, resulting in the disruption of the helical structure and biochemical processes.[22]

On the other hand, 316L stainless steel (316L SS) is the most commonly used alloy in medical implants due to its good corrosion performance, notable biocompatibility, high mechanical properties and low cost accessibility.[23] According to this, in our laboratory a microstructured PPy film was electrosinthetized onto 316L SS from a solution containing copper species. The results indicated that PPy/Cu-modified electrodes are effective for water disinfection contaminated with *E. coli*.[14] Furthermore, it has been demonstrated that a salicylate-doped PPy film is an effective matrix for immobilizing Ag species, and the resulting composites exhibit excellent performance in inhibiting the activity of *S. aureus* bacteria. These findings suggest that the composite holds promise for biomedical applications.[16]

Considering the advantages of silver and copper species, as well as the synergistic effect of these metals with PPy in antibacterial studies, the aim of this research is to study the bactericidal effect of copper–polypyrrole composites modified with silver nanoparticles deposited on 316L SS. According to the bibliography consulted, this study is the first to evaluate the antibacterial properties of a PPy composite against a total of twenty-four strains of both Gram-positive and Gram-negative bacteria. These isolates include reference strains (*E. coli* ATCC 25922, *E. coli* 0157:H7 EDL 933, *S. aureus* ATCC 25923 and *Listeria monocytogenes* ATCC 7644) and strains isolated from food and clinical samples. Given the extensive range of bacteria examined, the resulting composite shows promise as a surface modification material for 316L SS, with potential applications in various fields such as medical instruments, water treatment devices, and food processing.

EXPERIMENTAL

Chemicals

Pyrrole (99.9 % purity), silver nitrate (99.9 % purity) and sodium salicylate (99.9 % purity) were obtained from Sigma. Copper sulphate pentahydrate (98 % purity) and potassium nitrate (98 % purity) were obtained from Cicarelli Laboratorios (Santa Fe, Argentina). Pyrrole (Sigma–Aldrich) was freshly distilled under reduced pressure prior to use.

Bacterial strains

The antibacterial properties of composites were tested against four reference strains (*Escherichia coli* ATCC 25922, *E. coli* 0157:H7 EDL 933, *Staphylococcus aureus* ATCC 25923 and *Listeria monocytogenes* ATCC 7644), four *E. coli* strains (named 6, 17, 19 and 28) isolated from recreational waters,[24] thirteen *S. aureus* strains (named 1 and 13) obtained from the nose of asymptomatic volunteers, *Pseudomonas aeruginosa* isolated from drinking water and *Salmonella* spp. and *Listeria innocua* isolated from meat products.

Electrosynthesis and characterization of composite

The composites were electrosynthesized onto 316L SS sheets (wt. %: 17.47 Cr, 10.32 Ni, 1.88 Mn, 1.90 Mo, 0.39 Si, 0.025 C and Fe balance) with an exposed area of 0.25 cm^2. Prior to each experiment, the exposed 316L SS surface was abraded with a 1200-grit finish using SiC, then degreased with acetone, and finally washed with triply distilled water. For the electrochemical experiments, a conventional three-electrode system and a 20 cm^3 Metrohm cell were used. A Pt sheet served as the counter electrode, while a commercially available Ag/ /AgCl/3M KCl electrode (Metrohm) was used as the reference electrode. All potentials are referred to Ag/AgCl scale.

As described in our earlier work, PPy films and copper–PPy (Cu–PPy) composites were obtained potentiostatically at 0.90 V from a solution containing 0.25 M pyrrole + 0.50 M Na salicylate. In the case of the Cu–PPy composite, a concentration of 0.10 M $CuSO_4 \cdot 5H_2O$ was also incorporated in the electrosynthesis solution.[15] Silver nanoparticles were electrodeposited onto PPy and Cu–PPy using a solution containing $AgNO_3$ + KNO_3, following the potentiostatic double-pulse technique introduced by Scheludko and Todorova.[25] The process is based on the following parameters: nucleation potential E_1 = –0.8 V for nucleation time t_1 = 0.5 s and growth potentials of E_2 = 0.1 V for growth time t_2 = 30 s. The size of the nanoparticles was controlled by the solution concentration.

Electrochemical experiments were performed using a potentiostat–galvanostat Autolab PGSTAT128 N. Morphological studies of gold metallized films were conducted using a scanning electron microscopy (SEM), specifically the LEO 1450 VP system, which was equipped with an energy-dispersive scanning (EDS) probe. Additionally, the electrical conductivity of the films was measured using a homemade device through the two-probe method.

Disk diffusion assay

The antimicrobial effectiveness of the coatings was tested using the Kirby-Bauer disk diffusion method, following the model of antibiogram execution.[26]

Briefly, cultures of the strains under study were cultivated on Muller–Hinton agar (MHA) plates from Britania Laboratories S.A., Argentina, for 24 h at 37 °C. The resulting colonies were suspended in Muller–Hinton broth from the same manufacturer. The turbidity (expressed as optical density; *OD*) of the bacterial suspensions was measured using an optical spectrophotometer (λ = 600 nm). The suspensions were adjusted to a turbidity of 0.5 based on the McFarland standard (10^6 CFU mL^{-1}). A sterilized cotton swab was dipped into the resulting suspension, and used to apply a bacterial lawn on MHA plates. Petri plates were left to dry for 10 min, after which the composites were distributed, using the bare alloy and the PPy covered electrode as control samples. Incubation was carried out at 37 °C, and after 24 h, the plates were examined to identify the presence or absence of zones of inhibition. When zones of inhibition were observed, their diameter was measured with a ruler with a resolution of up to 1 mm. For each type of composite and microbial strain, the mean and standard deviation (*SD*) were calculated based on data obtained from two independent replicates.

RESULTS AND DISCUSSION

Electrosynthesis and characterization of composites

The formation and characterization of PPy and Cu–PPy coatings on 316L SS were discussed in our prior work.[15] As mentioned before, both films have a morphology composed of hollow rectangular-sectioned microtubes. The proposed mechanism for the formation of these microtubes consists in the early crystallization of salicylic acid (HSa) on a granular PPy. These crystals are formed due to the rapid production of H^+, which protonate the salicylate anions, constituting the building blocks for the formation of the rectangular microtubes.[27]

Firstly, the electrodeposition of silver nanoparticles onto PPy was performed using the potentiostatic double-pulse technique. The initial pulse is applied to facilitate the formation of nuclei, while the subsequent pulse, with a more positive potential than the first one, regulates the growth of the nuclei deposited during the preceding pulse.[25]

To control the nanoparticles size, two solutions with different concentrations were used: For smaller nanoparticles, a solution with a concentration of 5 mM $AgNO_3$ + 50 mM KNO_3 was utilized. SEM/EDS analysis was performed to characterize the composite. In Fig. 1a, it can be observed that the surface of the PPy film is effectively decorated with AgNps, approximately 100 nm in size. EDS spectra (Fig. 1b) were used to demonstrate the presence of metallic silver, with the signal typically appearing between 3–3.6 keV.[28] The weight percentage registered for this element was 6.8 %. The spectrum also displayed signals of C and O associated with organic compounds.[29] In order to increase the size of the deposits on the PPy films, the concentration of the electrosynthesis solution was raised to 10 mM $AgNO_3$ + 100 mM KNO_3. As seen in Fig. 1c, nanoparticles of approximately 500 nm were obtained. In this case, the EDS analysis (Fig. 1d) shows a signal indicating the presence of metallic silver, with a content of 13.8 wt. %. The results demonstrated a direct correlation between the increase in Ag weight percentage and the increment in the particle size. To facilitate comprehension, the obtained composites were named PPy/$AgNp_{100}$ and PPy/$AgNp_{500}$, according to the nanoparticle size. Regardless of the AgNps size, a rosette-like structure characterizes most of the deposits. These preliminary findings indicate that, when applying the same electrochemical procedure, a rise in the concentration of the electrosynthesis solution, would not only lead to a growth in nanoparticle size but also to an increase in the amount of metallic silver in the composites.

To verify the amount of metallic silver deposited in the composites, a cyclic voltammetry experiment was performed. The procedure involved cycling the electrodes, which were covered with PPy/AgNp100 and PPy/AgNp500 in a 0.25 M Na salicylate solution between the potentials of –0.60 and 1.20 V at 0.01 V s–1. The polymer without nanoparticles was also cycled. Fig. 2 illustrates that the electro-

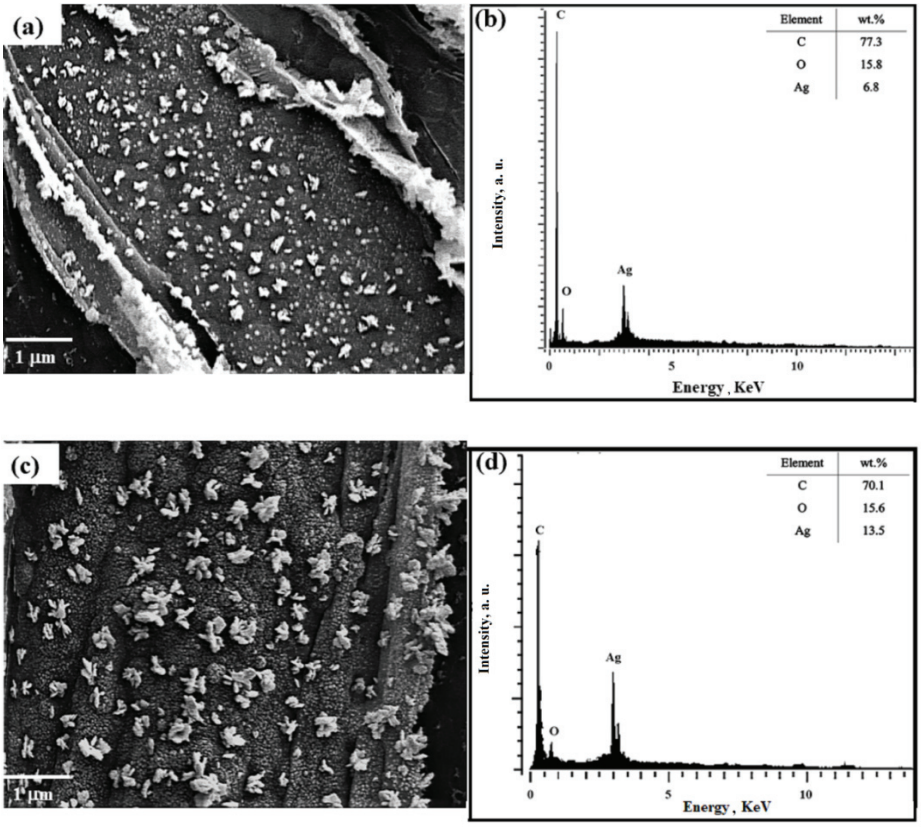

Fig. 1. SEM images and EDS spectra of PPy/AgNp100 (a, b) and PPy/AgNp500 (c, d).

chemical behavior of the composites differs significantly depending on the size of the silver nanoparticles. The strong and well-defined anodic peaks at 0.50 V are a result of the oxidation process of the deposited metal.[16] For the PPy/ /$AgNp_{500}$ composite, the oxidation peak is associated with a current density of 6.5 mA/cm^2 (see curve b), while for the PPy/$AgNp_{100}$ composite, the oxidation peak is associated with a current density of 2.5 mA/cm^2 (see curve a). The peak area analysis of the oxidative peaks reveals that, as the nanoparticle size increases, the peak area also increases, indicating a higher concentration of metallic silver in the composite. Moreover, at approximately 1.0 V, a peak associated with the overoxidation of the polymer is observed in both composites.[30] In the reverse scan, cathodic peaks appear at 0.0 V, indicating the reduction of silver ions. Based on the comparison of the current density of reduction peaks, it can be concluded that a higher amount of silver ions redeposited back into the composites is associated with a larger size of AgNps. In contrast, regarding unmodified PPy, no peak is observed in this potential range (curve c).

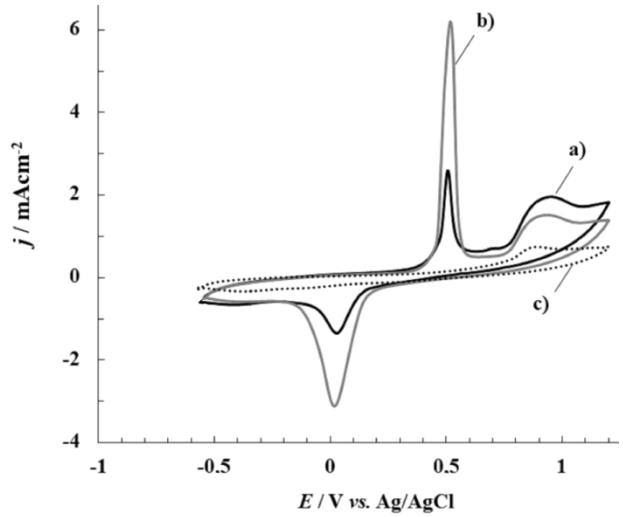

Fig. 2. Cyclic voltammograms registered in a 0.25 M Na salicylate solution at 0.01 V s^{-1} for 316L SS electrode coated with: a) $PPy/AgNp_{100}$ and b) $PPy/AgNp_{500}$. The data for unmodified PPy coated-316L SS is also provided (curve c).

With the aim of determining the amount of silver deposited in the composites, conductivity was measured. The values obtained were 28 S m^{-1} for PPy/ /AgNp100 and 42 S m^{-1} for $PPy/AgNp_{500}$. These values fall within the range already reported for conductive polymers modified with nanoparticles.[31] In the case of unmodified PPy, the conductivity value was 3.8 S m^{-1}. These values were estimated based on a film thickness of 7 μm.[32] Firstly, it can be observed that the incorporation of silver nanoparticles contributes to the improvement of the electrical conductivity of the PPy films.[28] The difference between the conductivity values of $PPy/AgNp_{100}$ and $PPy/AgNp_{500}$ could be attributed to the size of AgNps deposited in the composites. It is worth noting that an increase in the conductivity of the composites is associated with an augment of metallic silver deposited on the polymer. Indeed, Diantoro *et al.* proved conclusively that increased quantities of AgNps integrated into a conducting polymer enhance the conductivity of the composite.[33]

Considering the excellent results obtained in water disinfection with Cu–PPy films,[15] we decided to deposit AgNps onto Cu–PPy to study the antibacterial influence of both metals. In this process, silver nanoparticles were electrodeposited on Cu–PPy films, using the previously described double-pulse technique. The silver nanoparticles were obtained from a solution containing 10 mM $AgNO_3$ + 100 mM KNO_3. SEM micrograph of the polymer surface confirms the presence of PPy microtubes decorated with approximately 500 nm-sized AgNps (Fig. 3a). The magnified image shows that most of the nanoparticles have rosette-like structures (Fig. 3b). In this case, the composite was named $Cu–PPy/AgNp_{500}$.

EDS spectra confirm the presence of Ag and Cu in the composite, with respective contents of 4.7 and 4.9 wt. %. The signals of C and O correspond to the polymer composition, as expected.

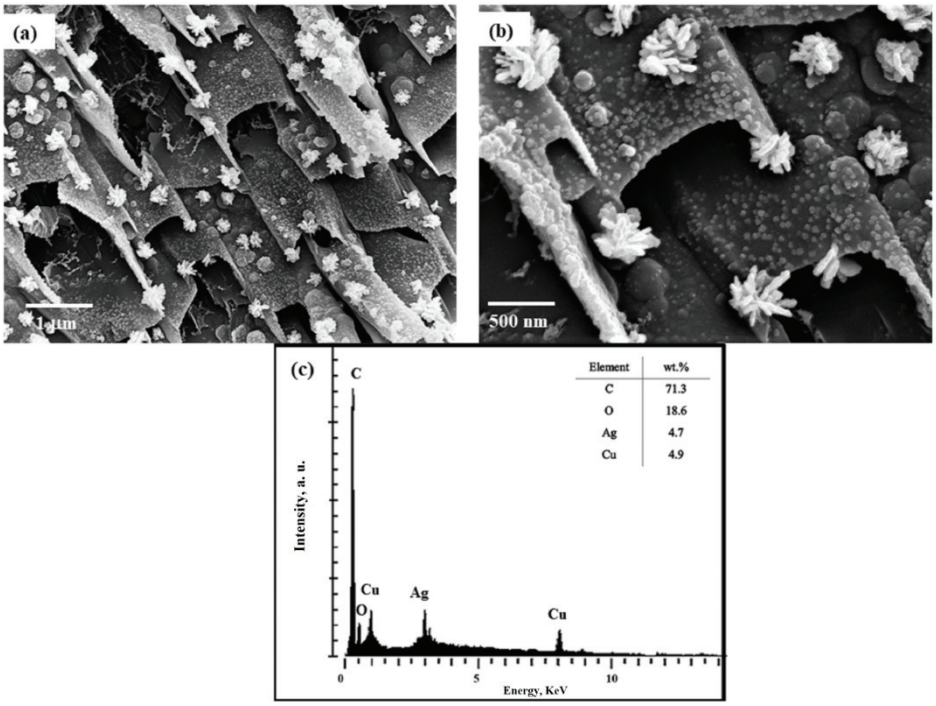

Fig. 3. SEM images (a, b) and EDS spectra (c) of Cu–PPy/$AgNp_{500}$.

To evaluate the chemical state of copper in the Cu–PPy and Cu–PPy/ /$AgNp_{500}$ composites, a cyclic voltammetry experiment was performed in a 0.25 M Na salicylate solution. In Fig. 4, the incorporation of Cu^{2+} is evidenced, in both films, by the presence of cathodic peaks at a potential of about –0.10 V, which are attributable to ion reduction.[15] In the case of Cu–PPy/$AgNp_{500}$, an overlap of Ag^{+} and Cu^{2+} reduction peaks is registered. The inset in Fig. 4 shows the anodic peaks of copper metal dissolution in both composites. As it was expected, the presence of a strong and well-defined anodic peak at 0.50 V is showed for Cu–PPy/$AgNp_{500}$ as a result of the oxidation process of the AgNps (curve b). In this case, the current density associated with the oxidation peak of the silver nanoparticles is 6.0 mA/cm^2, a similar value to the one obtained previously. On the other hand, no peak is observed for the Cu–PPy composite (curve a) in this potential range.

XPS analysis was used to determine the specific electron binding energies of the elements on the surface of the composites. Fig. 5 displays the survey spectra of

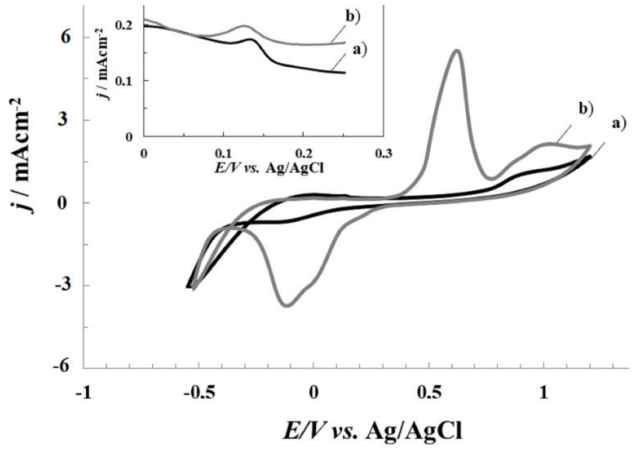

Fig. 4. Cyclic voltammograms registered in a 0.25 M Na salicylate solution at 0.01 V s^{-1} for 316L SS electrode coated with: a) Cu–PPy and b) Cu–PPy/$AgNp_{500}$. The inset shows the curves amplified.

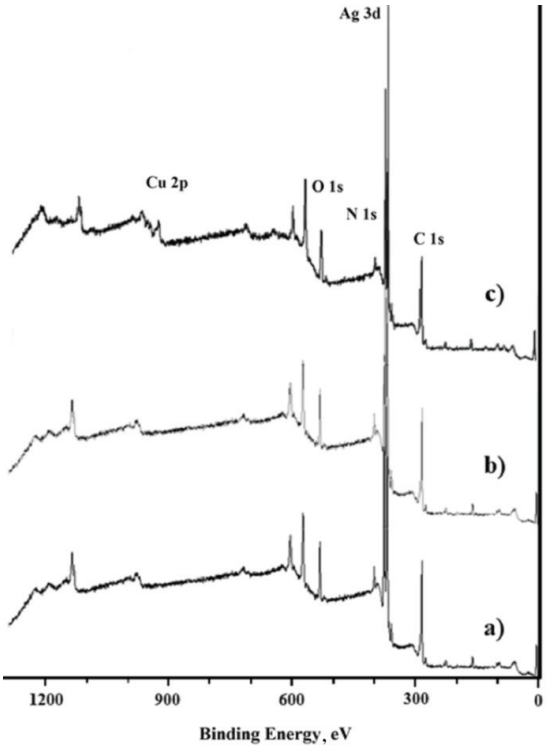

Fig. 5. XPS survey spectra of: a) PPy/$AgNp_{100}$, b) PPy/$AgNp_{500}$ and c) Cu–PPyAgNp_{500}.

the composites PPy/$AgNp_{100}$, PPy/$AgNp_{500}$ and Cu–PPyAgNp_{500}. The elements detected in all composites are C 1s, O 1s and N 1s, since they are the main

components of the polypyrrole matrix and the dopant (Sa/HSa).[22] In Fig. 6a, the high-resolution spectrum of Ag 3d is presented. As can be seen, this element is also present in all samples. The two significant XPS signals, located at approximately 374.2 and 368.2 eV and separated by a distance of 6.0 eV, correspond to the Ag $3d_{3/2}$ and Ag $3d_{5/2}$ binding energies of Ag, respectively.[34] The results indicate the successful reduction of silver ions to zero-valent silver nanoparticles during the double pulse technique. On the other hand, the existence of Cu^{2+} is detected solely in the XPS survey of Cu–PPyAgNp$_{500}$ (Fig. 5, curve c), which is consistent with the Cu 2p signal. In Fig. 6b, the peaks at approximately 935.3 and 955.3 eV are assigned to Cu $2p_{3/2}$ and Cu $2p_{1/2}$, respectively, while the peaks in the range of 940–945 eV and 964.1 eV correspond to the shake-up satellite peaks of Cu 2p, as supported by previous research.[35,36] The XPS characterization supports the hypothesis that the polymer matrix contains Cu^{2+}, as postulated in our previous study, where the presence of cathodic peaks during potentiodynamic polarization (Fig. 4) was attributed to ion reduction.[15]

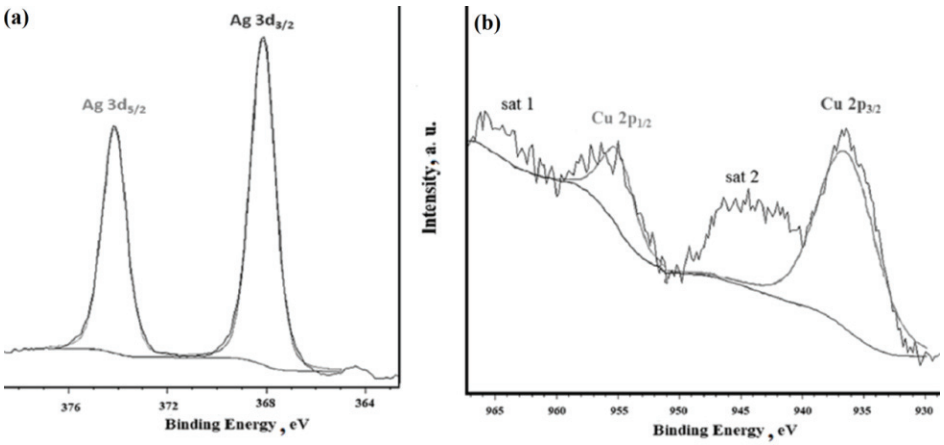

Fig. 6. XPS spectra of Cu–PPyAgNp500: Ag 3d (a) and Cu 2p (b).

Agar diffusion assay

In order to assess the *in vitro* antibacterial efficacy of the resulting composites, the agar diffusion method was employed. The diameter of inhibition zones (DIZ) after 24 h is shown in Fig. 7.

Overall, Cu–PPy/AgNp$_{500}$ exhibited antibacterial activity against the majority of the species tested (23/24). This composite proved effective against all *S. aureus* strains and all Gram-negative bacteria under investigation. While several studies suggest that Gram-positive *S. aureus* is more resistant to silver nanoparticles compared to Gram-negative *E. coli*,[37–39] this result does not consistently hold true.[40]

PPy/AgNp$_{500}$ and Cu–PPy/AgNp$_{500}$ had a significant impact on the cellular viability of *S. aureus*, *E. coli*, *S. enterica*, *L. innocua* and *P. aeruginosa*. However, no activity was observed on the growth of *L. monocytogenes* ATCC 7644, which was only inhibited by PPy/AgNp$_{100}$.

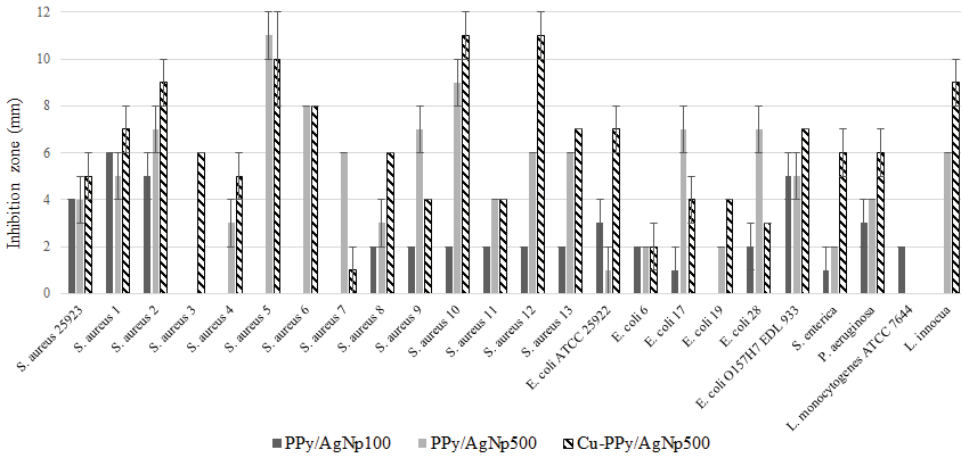

Fig. 7. Growth inhibition of different microbial species by copper and silver ions released from a coated specimen.

In particular, compared to PPy/AgNp$_{100}$, PPy/AgNp$_{500}$ and Cu–PPy/AgNp$_{500}$ exhibited higher antimicrobial activity against *S. aureus* strains 3, 8 and 12; *E. coli* ATCC 25922; *E. coli* strain 19; *S. enterica*; *P. auruginosa*; *L. innocua*.

Given the nature of the agar diffusion method, which involves measuring the diameter of inhibition zones (*DIZ*) on agar plates using a ruler with a resolution of 1 mm, it is important to acknowledge the possibility of measurement errors. However, this method demonstrates the potential antibacterial effect of composites against various microbial strains. In the agar diffusion method, the *DIZ* surrounding a composite serves as an indicator of the microorganisms' sensitivity to the composite. While studies reporting *DIZ* values offer a quantitative measure of antibacterial activity, there is still significant non-uniformity in the experimental methods employed. The *DIZ* can exhibit variability, even within the context of the same microbial strain exposed to silver/copper composites. These variations may be attributed to several factors, including variations in the growth medium, differences in the initial concentration of microorganisms, and the size, shape and composition of nanoparticles. Thus, comparing the sensitivity of different strains to copper or silver nanocomposites is often not feasible, despite the wealth of available literature on the topic.[41]

Most research on bactericidal effects of silver and cooper has been limited to a small number of microbial strains or, in some cases, only a single strain. However, this study sought to compare the antibacterial effects of silver and copper compounds across a wider spectrum of twenty-four bacterial strains. These strains included four reference strains, five strains isolated from water sources, thirteen strains obtained from human clinical samples and two strains isolated from food sources. The findings of this study revealed strain-specific characteristics, which can eventually contribute to the improved and effective utilization of these compounds for specific applications.

In recent years, numerous interconnected investigations have been conducted to enhance the utilization of AgNps for bacteria inhibition. However, an ongoing debate persists regarding the antibacterial action mechanism of AgNps. Previous studies have indicated that the bactericidal properties of AgNps are primarily attributed to a two-step mechanism. Firstly, Ag^+ ions are released from the surfaces of nanoparticles. Subsequently, the released Ag^+ interacts with cellular targets, resulting in their bactericidal effect.[42]

The cellular uptake of AgNps is another mechanism associated with physical interaction, and occurs when Nps are small enough to cross the cell membrane.[43] Mukha *et al.* showed that the antibacterial activity of AgNps smaller than 10 nm is attributed to both membrane damage and their ability to penetrate into the cell.[44] Similarly, Dong *et al.* evaluated Nps of varying sizes and reached the conclusion that AgNps of smaller dimensions are more effective due to their ability to pierce the cell membrane.[45] In a separate study, Oves *et al.* synthesized AgNps with bacterial exopolysaccharides, spherical shape, and a size of about 35 nm.[46] They demonstrated that the antimicrobial activity of these Nps against *B. subtilis* and methicillin-resistant *S. aureus* (MRSA) is attributed to ROS production within bacterial cells. It has been suggested that AgNps smaller than the pore size can easily penetrate the pore networks and efficiently depolarize the inner membrane, causing a bactericidal effect.[47] In general, bacterial cells have a size in the micrometer range, whereas their outer cell membranes feature pores measuring in the nanometer range (<50 nm). Since AgNps used in this study are larger than the pores of the outer cell membrane, they are unable to penetrate the cell membrane. Conversely, the higher antibacterial efficacy of PPy/$AgNp_{500,}$ in contrast with PPy/$AgNp_{100}$, can be attributed to the larger amount of ionic silver released as a result of the larger nanoparticle size.

The antibacterial activity of Cu–PPy/$AgNp_{500}$ composites encompasses a series of steps. One of these steps involves the dissolution of AgNps to release silver ions, along with the diffusion of copper ions from the PPy matrix. The release of silver ions leads to the disruption of the cytoplasm and the cell wall, while also triggering the production of ROS. This ROS production by respiratory enzymes inhibits the release of adenosine triphosphate.[48] It is possible that the

mechanism underlying the antibacterial action of cooper ions may be attributed to the generation of ROS, which induces oxidative stress and/or damage in the bacteria.[49] In addition to ROS production, the cationic interaction of Ag^{+} and Cu^{2+} with negatively charged components of the bacteria cell membrane results in improved bactericidal efficacy at higher concentrations, achieved through the processes of cell lysis and bacteria collapse.[50] Hence, it is expected that both Cu and AgNps are able to interact with the entire surface of the bacterium. As a result, the copper and silver ions, which are toxic to bacteria, penetrate the cell wall, initiating a series of reactions that ultimately result in cell death.[51,22] Drawing on these findings, it can be suggested that the antimicrobial activity primarily stems from the presence of silver in AgNp, while the addition of copper ions further enhances its antibacterial efficacy. Consistent with this, Mujeeb *et al.* found that silver–copper nanocomposites (Ag–CuNCs), synthetized using an *Olax scandens* leaf extract, exhibited a greater antimicrobial activity than monometallic AgNps. Importantly, this enhanced antimicrobial activity was associated with an increase in the production of ROS.[52]

CONCLUSIONS

In the present study, PPy and Cu–PPy composites underwent electrochemical modification using two different sizes of AgNps. The results demonstrated that a higher concentration of metallic silver in the composite corresponded to a larger size of nanoparticles. Furthermore, it was found that the size of AgNps deposited on the PPy film influenced the antibacterial activity of the modified composites. It was proposed that the higher antibacterial efficacy of PPy/ /$AgNp_{500}$, compared to PPy/$AgNp_{100}$, can be attributed to a greater release of ionic silver resulting from the larger nanoparticle size. Although all PPy-modified films exhibited antibacterial properties, Cu–PPy/$AgNp_{500}$ emerged as the composite that exhibited the strongest antibacterial activity against most of the species tested. This heightened antibacterial activity can be largely ascribed to the synergistic potential of both metals for eradicating bacteria. The surface modification of 316L SS with these films holds promise as a viable alternative for the development of novel antibacterial composites capable of inhibiting the proliferation of large amounts of bacteria.

SUPPLEMENTARY MATERIAL

Additional data and information are available electronically at the pages of journal website: https://www.shd-pub.org.rs/index.php/JSCS/article/view/12276, or from the corresponding author on request.

Acknowledgements. The financial support provided by CONICET (2021-2023 GI--11220200102064CO), ANPCYT (PICT-2019-02758) and Universidad Nacional del Sur (PGI-UNS 24/M159), in Bahía Blanca, Argentina, are gratefully acknowledged.

ИЗВОД

БАКТЕРИЦИДНИ ЕФЕКАТ КОМПОЗИТА БАКАР–ПОЛИПИРОЛ МОДИФИКОВАНИХ НАНОЧЕСТИЦАМА СРЕБРА НА ГРАМ-ПОЗИТИВНЕ И ГРАМ-НЕГАТИВНЕ БАКТЕРИЈЕ

PATRICIA L. MARUCCI[1], MARIA G. SICA[1,2], LORENA I. BRUGNONI[1,3] и MARÍA B. GONZÁLEZ[4]

[1]*Department of Biology, Biochemistry and Pharmacy, National University of the South, Bahía Blanca, Argentina,* [2]*Department of Health Sciences, National University of the South, Bahía Blanca, Argentina,* [3]*Institute of Biological and Biomedical Sciences, National University of the South, CONICET, Bahía Blanca, Argentina and* [4]*Chemical Engineering Department, Institute of Electrochemistry and Corrosion Engineering, National University of the South, CONICET, Bahía Blanca, Argentina*

У раду је испитиван бактерицидни ефекат композита бакар–полипирол (Cu–PPy) таложених на нерђајући челик 316L и модификованих сребром. Процењена су антимикробна својства према двадесет четири соја Грам-позитивних и Грам-негативних бактерија. Међу двадесет четири проучавана соја, изолати су укључивали референтне сојеве (*Escherichia coli ATCC 25922*, *Escherichia coli 0157:H7 EDL 933*, *Staphylococcus aureus ATCC 25923* и *Listeria monocytogenes ATCC 7644*), као и сојеве изоловане из хране и клиничке узорке. Антимикробна активност композита показала је да сви филмови модификованог полипирола имају антибактеријска својства. Значајно је да је Cu–PPyAgNp$_{500}$ показао најјачу инхибиторну активност против Грам-негативних и Грам-позитивних бактерија. Модификација површине челика 316L овим филмовима је обећавајућа и одржива алтернатива за развој нових антибактеријских композита који могу инхибирати раст значајног броја бактерија.

(Примљено 13. фебуара, ревидирано 26. марта, прихваћено 2. августа 2023)

REFERENCES

1. World Health Organization (WHO), 2021, *Antimicrobial resistance*, Available from https://www.who.int/news-room/fact-sheets/detail/antimicrobial-resistance (accessed 26 October 2022)
2. World Health Organization (WHO), 2015, *Global Action plan antimicrobial resistance*, Document Production Services, Geneva, Switzerland. Available from https://ahpsr.who.int/publications/i/item/global-action-plan-on-antimicrobial-resistance (accessed 26 October 2022)
3. E. Seebach, K. F. Kubatzky, *Front. Immunol.* **10** (2019) 1724 (https://doi.org/10.3389/fimmu.2019.01724)
4. M. Z. Ibrahim, A. A. D. Sarhan, F. Y. M. Hamdi, *J. Alloys Compd.* **714** (2017) 636 (https://doi.org/10.1016/j.jallcom.2017.04.231)
5. N. F. Kamaruzzaman, L. P. Tan, R. H. Hamdan, S. S. Choong, W. K. Wong, A. J. Gibson, A. Chivu, M. de F. Pina, *Int. J. Mol. Sci.* **20** (2019) 2747 (https://doi.org/10.3390/ijms20112747)
6. K. Jlassi, M. H. Sliem, F. M. Benslimane, N. O. Eltai, A. M. Abdullah*, Prog. Org. Coat.* **149** (2020) 105918 (https://doi.org/10.1016/j.porgcoat.2020.105918)
7. M. Wang, and T. Tang, *J. Orthop. Transl*. **17** (2019) 42 (https://doi.org/10.1016/j.jot.2018.09.001)
8. M. Maruthapandi, A. Saravanan, A. Gupta, J. H. T. Luong, A. Gedanken*, Macromol.* **2** (2022) 78 (https://doi.org/10.3390/macromol2010005)
9. B. Balasubramaniam, Prateek, S. Ranjan, M. Saraf, P. Kar, S. P. Singh, V. K. Thakur, A. Singh, R. K. Gupta, *ACS Pharmacol. Transl. Sci*. **4** (2021) 8 (https://doi.org/10.1021/acsptsci.0c00174)

10. M. Talikowska, X. Fu, G. Lisak, *Biosens. Bioelectron*. **135** (2019) 50 (https://doi.org/10.1016/j.bios.2019.04.001)
11. E. N. Zare, T. Agarwal, A. Zarepour, F. Pinelli, A. Zarrabi, F. Rossi, M. Ashrafizadeh, A. Maleki, M. Shahbazi, T. K. Maiti, R. S. Varma, F. R. Tay, M. R. Hamblin, V. Mattoli, P. Makvandi, *Appl. Mater. Today* **24** (2021) 101117 (https://doi.org/10.1016/j.apmt.2021.101117)
12. A. Singh, A. Goswami, S. Nain, *Appl. Nanosci.* **10** (2020) 2255 (https://doi.org/10.1007/s13204-020-01394-y)
13. M. Balaji, P. Nithya, A. Mayakrishnan, S. Jegatheeswaran, S. Selvam, Y. Cai, J. Yao, M. Sundrarajan, *Appl. Surf. Sci.* **510** (2020) 145403 (https://doi.org/10.1016/j.apsusc.2020.145403)
14. M. B. González, D. O. Flamini, L. I. Brugnoni, L. M. Quinzani S. B. Saidman, *J. Water Health* **16** (2018) 921 (https://doi.org/10.2166/wh.2018.072)
15. M. B. González, L. I. Brugnoni, D. O. Flamini, L. M. Quinzani, S. B. Saidman, *Environ. Monit. Assess*. **189** (2017) 53 (https://doi.org/10.1007/s10661-016-5764-7)
16. M. B. González, L. I. Brugnoni, M. E. Vela, S. B. Saidman, *Electrochim. Acta* **102** (2013) 66 (https://doi.org/10.1016/j.electacta.2013.03.116)
17. A. Martinez, L. Brugnoni, D. Flamini, S. Saidman, *Prog. Org. Coat.* **144** (2020) 105650 https://doi.org/10.1016/j.porgcoat.2020.105650
18. Y. Qing, L. Cheng, R, Li, G. Liu, Y. Zhang, X. Tang, J. Wang, H. Liu, L. Qin, *Int. J. Nanomed*. **13** (2018) 3311 (http://dx.doi.org/10.2147/IJN.S165125)
19. K. M. Rice, G. K. Ginjupalli, N. D. P. K. Manne, C. B. Jones, E. R. Blough, *Nanotechnology* **30** (2019) 372001 (https://doi.org/10.1088/1361-6528/ab0d38)
20. T. V. Basova, E. S. Vikulova, S. I. Dorovskikh, A. Hassan, N. B. Morozova, *Mater. Des*. **204** (2021) 109672 (https://doi.org/10.1016/j.matdes.2021.109672)
21. D. Mitra, E. T. Kang, K. G. Neoh, *Appl. Mater. Interfaces* **12** (2020) 21159 (https://doi.org/10.1021/acsami.9b17815)
22. I. Salah, I. P. Parkin, E. Allan, *RSC Adv.* **11** (2021) 18179 (https://doi.org/10.1039/D1RA02149D)
23. Y. Zhuang, S. Zhang, K. Yang, L. Ren, K. Dai, *J. Biomed Mater. Res*., *B* **108** (2020) 484 (https://doi.org/10.1002/jbm.b.34405)
24. P. L. Marucci, N. L. Olivera, L. I. Brugnoni, M. G. Sica, M. A. Cubitto, *Environ. Monit. Assess*. **175** (2011) 1 (https://doi.org/10.1007/s10661-010-1488-2)
25. A. Scheludko, M. Todorova, *Bull. Acad. Bulg. Sci. Phys*. **3** (1952) 61
26. A. W. Bauer, W. M. Kirby, J. C. Sherris, M. Turck, *Am. J. Clin. Pathol.* **45** (1966) 493
27. M. B. González, O. V. Quinzani, M. E. Vela, A. A. Rubert, G. Benítez, S. B. Saidman, *Synth. Met.* **162** (2012) 1133 (http://doi.org/10.1016/j.synthmet.2012.05.013)
28. A. Alqudami, S. Annapoorni, P. Sen, R. S. Rawat, *Synth. Met.* **157** (2007) 53 (http://doi.org/10.1016/j.synthmet.2006.12.006)
29. M. B. González, S. B. Saidman, *Corros. Sci.* **53** (2011) 276 (https://doi.org/10.1016/j.corsci.2010.09.021)
30. R. Holze *Polymers* **14** (2022) 1584 (https://doi.org/10.3390/polym1408158 4)
31. Q. Pei, R. Qian, *Electrochim. Acta* **37** (1992) 1075 (https://doi.org/10.1016/0013-4686(92)85225-A)
32. A. Singh, Z. Salmi, N. Joshi, P. Jha, A. Kumar, H. Lecoq, S. Lau, M. M. Chehimi, D. K. Aswal, S. K. Gupta, *RSC Adv.* **3** (2013) 5506 (https://doi.org/10.1039/C3RA22981E)

33. M. Diantoro, T. Suprayogi, U. Sa'adah, N. Mufti, A. Fuad, A. Hidayat, H. Nur, in *Silver Nanoparticles*, K. Maaz, Ed., InTech, Rijeka, 2018 (https://doi.org/10.5772/intechopen.75682)
34. K. F. Babu, P. Dhandapani, S. Maruthamuthu, M. A. Kulandainathan*, Carbohydr. Polym*. **90** (2012) 1557 (https://doi.org/10.1016/j.carbpol.2012.07.030)
35. N. Song, S. Chen, D. Tian, Y. Li, C. Wang, X. Lu, *Mat. Today Chem.* **18** (2020) 100374 (https://doi.org/10.1016/j.mtchem.2020.100374)
36. J. Shu, Z. Qiu, S. Lv, K. Zhang, D. Tang, *Anal. Chem.* **89** (2017) 11135 (https://doi.org/10.1021/acs.analchem.7b03491)
37. B. Chudasama, A. K. Vala, N. Andhariya, R. V. Mehta, R. V. Upadhyay, *J. Nanopart. Res.* **12** (2010) 1677 (https://doi.org/10.1007/s11051-009-9845-1)
38. J. S. Kim, E. Kuk, K. N. Yu, J. Kim, S. J. Park, H. J. Lee, S. H. Kim, Y. K. Park, Y. H. Park, C. Hwang, Y. Kim, Y. Lee, D. H. Jeong, M. Cho, *Nanomed.: Nanotechnol. Biol. Med.* **3** (2007) 95 (https://doi.org/10.1016/j.nano.2006.12.001)
39. J. Jain, S. Arora, J. M., P. Omray, S. Khandelwal, K. M. Paknikar, *Mol. Pharm.* **6** (2009)1388 (https://doi.org/10.1021/mp900056g)
40. J. P. Ruparelia, S. P. Duttagupta, A. K. Chatterjee, S. Mukherji, *Acta Biomater.* **4** (2008) 707 (https://doi.org/10.1016/j.actbio.2007.11.006)
41. D. Longano, N.Ditaranto, L. Sabbatini, L. Torsi, N. Cioffi, in *Nano-Antimicrobials*, N. Cioffi, M. Rai, Eds., Springer, Berlin, 2011, pp. 85–117 (https://doi.org/10.1007/978-3-642-24428-5_3)
42. G. A. Sotiriou, A. Meye, J. T. Knijnenburg, S. Panke, S. E. Pratsinis, *Langmuir* **28** (2012) 15929 (https://doi.org/10.1021/la303370d)
43. J. S. McQuillan, A. M. Shaw, *Nanotoxicology* **8** (2014) 177 (https://doi.org/10.3109/17435390.2013.870243)
44. I. P Mukha, A. M. Eremenko, N. P. Smirnova, A. I. Mikhienkova, G. I. Korchak, V. F. Gorchev, A. Y. Chunikhin, *Appl. Biochem. Microbiol.* **49** (2013) 199 (http://doi.org/10.1134/S0003683813020117)
45. Y. Dong, H. Zhu, Y. Shen, W. Zhang, L. Zhang, *PLoS ONE* **14** (2019) e0222322 (https://doi.org/10.1371/journal.pone.0222322)
46. M. Oves, M. A. Rauf , A. Hussain, H. A. Qari, A. A. P. Khan, P. Muhammad, M. T. Rehman, M. F. Alajmi, I. L. M. Ismail, *Front. Pharmacol*. **10** (2019) 801 (https://doi.org/10.3389/fphar.2019.00801)
47. J. R. Morones-Ramirez, J. A. Winkler, C. S. Spina, J. J. Collins. *Sci. Transl. Med.* **5** (2013) 190ra81 (https://doi.org/10.1126/scitranslmed.3006276.)
48. S. Khorrami, A. Zarrabi, M. Khaleghi, M. Danaei, M. R. Mozafari, *Int. J. Nanomed.* **13** (2018) 8013 (https://doi.org/10.2147/IJN.S189295)
49. G. Applerot, J. Lellouche, A. Lipovsky, Y. Nitzan, R. Lubart, A. Gedanken, E. Banin, *Small* **8** (2012) 3326 (https://doi.org/10.1002/smll.201200772)
50. L-U. Rahman, A. Shah, S. K. Lunsford , C. Han, M. N. Nadagoud , E. Sahle-Demessie , R. Qureshi , M. S. Khan, H-B Kraatz, D. D. Dionysiou. *RSC Adv.* **5** (2015) 44427 (https://doi.org/10.1039/C5RA03633J)
51. T. V. Basova, E. S. Vikulova, S. I. Dorovskikh, A. Hassan, N. B. Morozova, *Mater. Des*. **204** (2021) 109672 (https://doi.org/10.1016/j.matdes.2021.109672)
52. A. Mujeeb, N. A. Khan, F. Jamal, K. F. Badre Alam, H. Saeed, S. Kazmi, A.W.F.Alshameri, M. Kashif, I. Ghazi M. Owais*, Front. Chem.* **8** (2020) 103 (https://doi.org/10.3389/fchem.2020.00103).